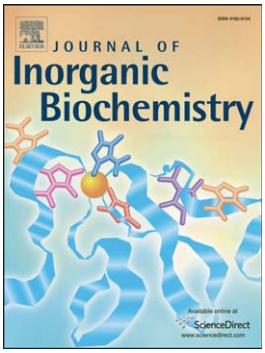

Tyrosine nitration in peptides by peroxynitrite generated *in situ* in a light-controlled platform: Effects of pH and thiols

Tara R. deBoer, Rafael I. Palomino, Sharon O. Idiga, Glenn L. Millhauser, Pradip K. Mascharak

PII: S0162-0134(14)00123-8
DOI: doi: 10.1016/j.jinorgbio.2014.04.018
Reference: JIB 9518

To appear in: *Journal of Inorganic Biochemistry*

Received date: 31 January 2014
Revised date: 25 April 2014
Accepted date: 28 April 2014

Please cite this article as: Tara R. deBoer, Rafael I. Palomino, Sharon O. Idiga, Glenn L. Millhauser, Pradip K. Mascharak, Tyrosine nitration in peptides by peroxynitrite generated *in situ* in a light-controlled platform: Effects of pH and thiols, *Journal of Inorganic Biochemistry* (2014), doi: 10.1016/j.jinorgbio.2014.04.018

Tyrosine nitration in peptides by peroxynitrite generated *in situ* in a light-controlled platform: Effects of pH and thiols

Tara R. deBoer, Rafael I. Palomino, Sharon O. Idiga, Glenn L. Millhauser, and Pradip K. Mascharak*

Department of Chemistry and Biochemistry
University of California Santa Cruz, Santa Cruz, CA 95064

*Corresponding author: Tel 1-831-459-4251
FAX: 1-831-459-2935
E-mail address: pradip@ucsc.edu

Keywords: Photoactive metal nitrosyl, Peroxynitrite, Nitric oxide, Superoxide, Tyrosine nitration

Highlights:

- Peroxynitrite was generated *in situ* within wells of a light-controlled platform
- A photoactive metal nitrosyl complex provides the optimal NO flux
- Effective tyrosine nitration in model peptides were demonstrated
- The platform allowed studies under different pH, CO_2 and thiol concentrations
- A cysteine neighbor strongly attenuates the extent of tyrosine nitration

ABSTRACT

Peroxynitrite has been shown to play a critical role in inflammation and affords 3-nitrotyrosine as the hallmark product. The reported methods of generating this reactive nitrogen species *in situ* often fails to provide a high and steady flux of peroxynitrite resulting in poor yields of 3-nitrotyrosine. Herein we report a two-component peroxynitrite-generating platform in which this anion is produced in a biomimetic fashion and under the control of visible light. Incorporation of the nitric oxide- and superoxide-generating components in polymer matrices allows easy alterations of pH in the reaction wells of this platform. We have demonstrated very efficient nitration of tyrosine by peroxynitrite at different pH values and with varying concentrations of carbonate. In addition to tyrosine, a set of tyrosine-containing peptides was also studied. Presence of glutathione in the reaction wells increases the extent of tyrosine nitration in such peptide substrates presumably by raising the lifetime of nitric oxide in the reaction medium. When a cysteine residue was included in the sequence of the peptide, the extent of nitration of the tyrosine residue was found to depend on the position of the cysteine residue with respect to tyrosine. The extent of tyrosine nitration is strongly attenuated when the cysteine residue is directly adjacent to the tyrosine. This effect has been attributed to an intramolecular radical transfer mechanism. Taken together, results of this study demonstrate the potential of this light-controlled platform as a convenient bioanalytical tool in studying the reactions of peroxynitrite under widely varying conditions.

1. Introduction

Peroxynitrite ($ONOO^-$, PN) is a short-lived reactive nitrogen species (RNS) that is generated from precursor radicals nitric oxide (NO) and superoxide ($O_2^{\bullet-}$) at a diffusion-controlled rate [1-6]. It is estimated that under pro-inflammatory conditions, this reactive anion is produced at a rate of 50-100 μM per min in cellular compartments [4]. Further, steady state concentrations of PN in the nanomolar range can persist under such conditions for hours. The reactive nature of this species contributes to a diverse chemistry implicated in a wide range of diseased states from Alzheimer's to atherosclerosis [7-13].

The product 3-nitrotyrosine (3-NT) has been identified as a hallmark footprint of PN *in vivo*, following the seminal work by Beckman and coworkers [14-16]. In general, nitration of a tyrosine residue is a selective process that can effectively modify the activity of biomolecules such as enzymes and proteins to induce inauspicious effects [1,3,17-20]. The mechanism of tyrosine nitration by PN is a highly dynamic reaction that is strongly affected by numerous factors including pH and CO_2 concentration [2,21,22]. At physiological pH (pH 7.4), the anionic form of PN predominates (~80%) and reacts rapidly with CO_2 (present in mM concentrations) to yield the nitrosoperoxocarbonate intermediate ($ONOOCO_2^-$). A significant portion of this anion (~33%) undergoes homolysis to yield the strong oxidant carbonate radical ($CO_3^{\bullet-}$) and nitrating agent nitrogen dioxide ($^{\bullet}NO_2$), both of which participate in the nitration of tyrosine. The extent of nitration by this mechanism is strongly pH-dependent.

In earlier studies, investigation into PN-dependent nitration afforded contradictory results depending on the mode of PN synthesis [23-25]. Due to the transient nature of this reactive species, strongly alkaline stock solutions of PN are commonly synthesized to maximize its lifetime [26,27]. While bolus addition of this stock solution can easily be incorporated into

buffered solutions, PN rapidly isomerizes (to nitrate) and/or decomposes to other species [28]. Such instability prevents studies on the effects of prolonged exposure of a steady flux of PN (and its precursor radicals) on biological substrates [29]. Comparative studies to elicit nitration effects of PN generated by more biomimetic co-generative methods (instead of chemically synthesized sources) have also afforded divergent results due to difficulties in controlling such two-components systems [23,30].

In the present work, we employed a two-component multi-well PN-generating platform to demonstrate effective nitration of tyrosine by a sustained level of PN generated *in situ* under the control of light [31]. Within this system, tyrosine and tyrosine-containing model peptides were exposed to PN under different conditions to probe the effects of pH, glutathione (GSH), CO_2 concentrations, and relative ratios of precursors NO and $O_2^{\bullet -}$ on this nitration reaction. The multi-well feature of the applied platform allows for multiple studies to be completed in synchrony. In addition to systematically modifying the milieu within selected wells to observe

Figure 1 here

modifications to tyrosine nitration as a function of *intermolecular* effects, we designed three model peptides to estimate the *intramolecular* effect of a thiol on tyrosine nitration upon exposure to PN. Interestingly, the cysteine residue promoted slight enhancement when separated from the tyrosine residue by several amino acid residues while a strong inhibitory effect was observed when the two residues were next to each other.

2. Materials and Methods

2.1 Materials

All chemicals used were analytical or ACS grade and received from chemical suppliers, unless otherwise stated. Platform components tetramethyl orthosilicate (TMOS), hypoxanthine (HX), and xanthine oxidase (XO) were purchased from Sigma-Aldrich. All peptides synthesized were assembled on a Rink-amide ChemMatrix® resin purchased from Sigma-Aldrich, and required amino acids were purchased from AAPPTec.

2.2 Preparation of the PN-generating platform

Prefabricated 24-well plates were synthesized as previously described [31]. Five-fold increase of all components was required to compensate for the increased well size in the present work. In short, to a stock solution of hydrolyzed tetramethyl orthosilicate solution $[Mn(Papy_3)(NO)]ClO_4$ ($PaPy_3$= *N,N´*-bis(2-pyridylmethylamine-N-ethyl-2-pyridine-2-carboxamide, (Mn(NO)) [32] was added and allowed to stir until the nitrosyl was completely dissolved. A batch of 600μl of this stock Mn(NO) solution was then added to individual wells and allowed to dry and age for 1 week prior to use. The final Mn(NO)-encapsulated sol-gel discs (Mn(NO)•SG) were stored at 4 ^{o}C in the dark prior to use.

In a second 24-well plate, a batch of 800μl of a xanthine oxidase/catalase containing sol-gel (XO/CAT•SG) mixture were plated into individual wells and allowed to dry and age for 1.5 weeks. Prior to their use, these enzyme encapsulated sol-gel discs were washed three times and their activity was evaluated by electronic absorption spectroscopy [31]. Construction of the PN-generating platform was completed by adding a single Mn(NO) sol-gel disc to each well of a 24-well plate with XO/CAT•SG layered at the bottom (Fig. 1). Generation of PN within the wells was initiated with the addition of hypoxanthine (HX) and concomitant illumination of the plate with broadband light (10 mW, Electrofiberoptics Corporation 410 illumination). Because the photoactive metal nitrosyl exhibits photobands in both visible and UV regions, a broadband light

source was employed to trigger the release of NO. Optimization of NO release from the Mn(NO) sol-gel under exposure to this low power light source was completed using a NO electrode (Innovative Instruments) to assure 1:1 flux ratio of NO and $O_2^{\bullet-}$ within the wells of the platform [31]. The kinetics of PN formation within the individual wells was followed (quantitated to be 4.42 ± 0.22 μM per min) using the PN probe coumarin-7-boronic acid [33].

2.3 Peptide Synthesis and Purification

All peptides were synthesized using Fmoc synthesis on a Liberty 1 Peptide Synthesizer with Discover® microwave platform (CEM, Matthews, NC). The syntheses were performed on a 0.1 mmol scale, and monitored with PepDriver software. The deprotection of the Fmoc group was achieved using a solution of 20% piperidine in dimethylformamide (DMF). Solutions of 0.625 M diisopropylcarbodiimide and 1.25 M hydroxybenzotriazole in DMF were used to activate the carboxy-termini. All coupling reactions were performed at 4 equivalents of Fmoc-amino acid, and each amino acid was double coupled and capped with a 10% acetic anhydride solution. Fully synthesized peptides were washed with dichloromethane and split into two reaction vessels for cleavage.

A cleavage cocktail consisting of 15 mL of trifluoroacetic acid, 0.5 mL each of 1,2-ethanedithiol and liquefied phenol, and 1 mL of triisopropylsilane, was added to each vessel of dried resin and reacted for 2 h followed by filtration. The filtrate was added to 90 mL of cold, dry diethyl ether for precipitation. The precipitate was collected by centrifugation, and the ether was discarded. The resulting pellet was dissolved in 20 mL of 1:1 H_2O/acetonitrile (1% formic acid) and lyophilized.

Peptides were purified by reversed phase (RP)-HPLC on a Vydac (Hesperia, CA) preparative C18 column. Fractions were collected and analyzed by electron spray ionization mass

spectrometry (ESI-MS) on a Micromass (Wythenshawe, UK) ZMD mass spectrometer to confirm the correct molecular weight. Fractions containing the correct molecular weight were combined and lyophilized. Further purification was performed on a semi-preparative scale as needed (HPLC chromatogram of all synthesized peptide shown in Supplementary Information, Fig. S1 and Fig. S2). Peptides were quantified by their UV absorbance at 280 nm.

2.4 Circular Dichroism

Far-UV CD measurements were performed with an AVIV 60DS spectrophotometer using a 0.1 cm path length cuvette. Peptides were prepared at 150 μM concentration in 50 mM phosphate-buffered saline (PBS) at pH 7.4. Spectra were recorded from 260 to 200 nm with a step size of 1 nm, a bandwidth of 1.5 nm, and an averaging time of 8 s. An average of 16 scans was obtained for each spectrum.

3. Experiments

3.1 Nitration of free tyrosine by PN under varied pH conditions

In a prefabricated 24-well PN-generating plate, three wells were prepared under three pH conditions (0.01M phosphate buffer, pH 7.4, 7.0, and 6.5). To each well, stock solutions of tyrosine, $NaHCO_3$ and hypoxanthine were added to achieve a final concentration of 1 mM, 1.25 mM and 0.4 mM, respectively. Immediately following the addition of these stock solutions the multi-well plate was illuminated with a low power broadband light source and allowed to mix on a plate rocker for 30 min. Termination of the reaction was completed by simply removing the reaction mixture from the plate and then transferring the analyte into a 1 mL centrifuge tube. This solution was centrifuged down to ensure absence of free-floating particulates. Samples were

then analyzed by electronic absorption spectroscopy (Cary 5000 Spectrophotometer) and ESI-MS to confirm and quantitate 3-NT formation.

3.2 Nitration of tyrosine by PN within a model peptide

In a prefabricated 24-well PN-generating platform, investigation into the nitration of a model tyrosine-containing peptide (**Y1**, sequence AAAAAKKAAA**Y**AAAKK) by PN was performed (at pH 7.4) by preparing three wells with 0.25 mM of the peptide, 0.4 mM HX, and 4 mM $NaHCO_3$. The plate was allowed to undulate on a plate rocker for 30 min while being illuminated by a low power broadband light source. The well content was then transferred to a 0.5 mL Eppendorf tube, centrifuged, and then analyzed by electronic absorption spectroscopy and mass spectrometry. Additionally, the effect of CO_2 on this PN-dependent reaction was evaluated by modulating the concentration of $NaHCO_3$ (0 mM, 1.25 mM, and 4 mM) in wells prepared as described above.

3.3 Nitration of tyrosine by PN within Peptide Y1 in the presence of GSH

Similar to the experimental system described above, three wells were prepared with 0.25 mM of the peptide, 0.4 mM HX, and 4 mM $NaHCO_3$ and supplemented with glutathione (1 mM). After 30 min of undulation and illumination, the reactions was terminated and evaluated as discussed above.

3.4 Modification of cysteine within a model peptide

In a prefabricated 24-well PN-generating platform, investigation on the modification of a model cysteine-containing peptide (**C1**, sequence AAAAAKKAAA**C**AAAKK) by PN was performed by preparing three wells with 0.25 mM of the peptide, 0.4 mM HX, and 4 mM $NaHCO_3$. Solutions were treated and evaluated as discussed above. Additionally, control wells

were prepared where **C1** was exposed to NO only (these wells excluded HX). Cysteine nitrosylation was then quantified by electronic absorption spectroscopy (λ_{max}= 336 nm, ε= 920 $M^{-1}cm^{-1}$) and employed as a correction factor.

3.5 Nitration of tyrosine by PN within a model peptide containing cysteine

Three peptides were designed with varied relative distance between a cysteine and tyrosine residues: **CY1**, sequence AAA**C**AAAKKAAA**Y**AAAKK; **CY2**, sequence AAAKAAA**C**KAAA**Y**AAAKK; and **CY3**, sequence AAAKKAAA**CY**AAAKK. In the prefabricated 24-well PN-generating platform, the intramolecular effect of thiols on the nitration of tyrosine in these peptides by PN was monitored. Three wells were prepared with 0.25 mM of the peptide, 0.4 mM HX, and 4 mM $NaHCO_3$. Solutions were treated and evaluated as discussed above. Additional control studies were completed with peptide **CY1**, where the peptide was exposed to NO or $O_2^{\bullet-}$. All other previously described parameters and protocols were maintained in these studies unless otherwise noted. Control studies on the effects of NO or $O_2^{\bullet-}$ were performed by removing the Mn(NO)•SG or XO/CAT•SG disc from the wells.

The standard deviation values reported for the nitration studies described below (in well volume of 500 μl, pH 7.4) were calculated using results obtained from a minimum of three independent measurements. The nitration of both free tyrosine and the tyrosine-containing peptides where calculated based on the concentration of PN generated within the wells of the platform.

4. Results

4.1 Effects of pH on tyrosine nitration

In order to establish the utility of our two-component PN-generating platform as an alternative tool to study biochemical modifications induced by this RNS, we first attempted to monitor the

effect of pH on the nitration of free tyrosine by PN. The formation and quantification of 3-NT formed was first evaluated by electronic absorption spectroscopy (λ_{max} = 370 nm). Standard solutions of 3-NT were prepared to optimize the extinction coefficient of this species under the defined experimental conditions and calculated to be 4015 $M^{-1}cm^{-1}$. As predicted, it was observed that increased acidity of the well content from pH 7.4 to 7.0 to 6.5 resulted in a general diminution of tyrosine nitration by PN (Table 1). Additionally, the collected analytes were studied by mass spectrometry (ESI, positive ion mode), which corroborate 3-NT formation with the presence of the corresponding peak at 227 m/z $[M+H]^+$. Much like our previously reported studies, a peak corresponding to 3,3'-dityrosine (361 m/z) was also observed. However, the relative abundance of 3-NT was greater than that of the dimer under the defined conditions. Control studies were completed at pH 7.4 where the flux ratio of $NO:O_2^{\bullet-}$ was changed from 1:1 to 1:2. This flux alterations was implemented by simply incorporating a Mn(NO) sol-gel piece with one-half the nitrosyl compound loaded into the sol-gel matrix (7.25 mg) [31]. Such changes resulted in a near elimination in tyrosine nitration (Figure S4).

Table 1 here

*4.2 Nitration of Peptide **Y1** and effects of CO_2 and GSH*

To extend the biochemical complexity of the PN substrate within the prefabricated platform, we designed and synthesized a model peptide that contained a single tyrosine residue (**Y1**) amenable to nitration. Nitration of the single tyrosine residue within the random coiled (confirmed by CD) peptide was first verified by electronic absorption spectroscopy, with a peak centered at 370 nm indicating the formation of 3-NT (Fig. 2). Mass spectrometry confirmed the

presence of this modification with a mass increase of 46 Da ($-NO_2$) indicative of nitration of the model peptide ($[M+3H]^{3+}$ = 521 m/z).

Figure 2 here

Because PN-mediated nitration of tyrosine is dependent on CO_2, we modulated the $NaHCO_3$ concentration (source of CO_2) within three PN- generating wells and observed alterations in the extent of nitration of **Y1**. In line with other PN studies with peptides and proteins, 250 μM of **Y1** was employed in these studies. As anticipated, enhancement in nitration of the tyrosine residue within **Y1** was observed under increasing concentrations of CO_2, with a ~4.5-fold increase in nitration being observed when the concentration of $NaHCO_3$ was increased from 1.25 mM to 4.0 mM (Table 2).

Table 2 here

Next, to investigate the effects of antioxidants on the nitration of tyrosine within the designed peptide we added the biologically relevant antioxidant thiol GSH into the PN-generating wells. Incorporation of GSH (1 mM) did not inhibit tyrosine nitration within **Y1** and instead resulted in a slight (~1.1-fold, 39.2 ± 1.2%) enhancement. Analysis of the well content collected from this experiment by mass spectrometry revealed the selective nitration of **Y1**, indicated by the presence of a peak at 521 m/z. Although control studies performed in the absence of **Y1** showed a small peak at 353 m/z correlating to the nitration of GSH in addition to a moderately strong peak at 360 m/z $[M+Na]^+$ due to S-nitrosylated GSH, the presence of **Y1** in the well resulted in the peak at 360 m/z $[M+Na]^+$ only (Fig. 3).

Figure 3 here

4.3 Thiol-containing peptides and the effect of thiol on tyrosine nitration

The results of the **Y1** nitration study in the presence of GSH prompted us to design a series of cysteine-containing peptides (**C1**, **CY1, CY2,** and **CY3**) to investigate the effect(s) of a thiol residue on the nitration of a neighboring tyrosine within a peptide chain (Supplementary Information, Fig. S3). Following exposure of the control peptide **C1** to PN within the platform, the well content was collected and first analyzed by electronic spectroscopy. A peak at 336 nm was observed, corresponding to S-nitrosylation and/or S-nitration of the thiol residue. The sample was then processed by mass spectrometry and a prominent peak corresponding to a mass increase of 30 Da (−NO) confirmed the formation of the S-nitrosylated product.

Investigation into the intramolecular effects of a thiol on neighboring tyrosine residue nitration was completed using the model peptides **CY1**, **CY2**, and **CY3**, where the cysteine and tyrosine residues were separated by varied number of amino acids within the primary sequence (Table 3). When the cysteine and tyrosine residues were separated by eight (**CY1**) or four (**CY2**) non-reactive amino acids, a slight enhancement in tyrosine nitration was observed. However, placement of these residues directly adjacent to each other resulted in a dramatic attenuation of tyrosine nitration based on the absorbance at 370 nm corresponding to 3-NT formation within the respective peptides (Table 3).

Table 3 here

The mass spectrum of the analyte collected from these wells showed formation of distinct products. In case of **CY1** and **CY2** peptides, predominant peaks corresponding to mass additions of 30 Da and 46 Da were present, corresponding to respective S-nitrosylation and tyrosine-nitration of the peptides. A strong electronic absorption peak at 370 nm confirmed that the extent of tyrosine nitration was much higher than that of S-nitrosylation of the cysteine residue.

Interestingly, the mass spectrum of the content of the well where **CY3** was exposed to PN showed mass additions of 16 Da, 30 Da, and 46 Da corresponding to oxidation, S-nitrosylation and S-nitration of the peptide substrate (Fig. 4). The nitrosylation/nitration of the cysteine residue was indicated by a strong absorption band at 330 nm. In addition, the absorption at 370 nm arising from nitration of tyrosine was diminished significantly compared to those observed with **CY1** and **CY2**.

Figure 4 here

Finally, in order to verify that both NO and $O_2^{\bullet-}$ were required to promote tyrosine nitration, the peptide **CY1** was allowed to react with each species individually. When **CY1** was exposed to NO, a peak at 330 nm in the absorbance spectrum corresponding to S-nitrosylation was observed. In contrast, no absorption in the 300-600 nm region was noted when this peptide was exposed to $O_2^{\bullet-}$ (Fig. 5). No absorption corresponding to 3-NT (370 nm) was observed in both cases.

Figure 5 here

5. Discussion

In this work we have employed a light-activated biomimetic PN-generating platform [31] to study the chemistry of tyrosine nitration mediated by PN. This platform releases sustained fluxes of NO, $O_2^{\bullet-}$, and PN upon exposure to light and addition hypoxanthine. It also allows studies with PN under varied pH conditions. With alternative sources such as authentic PN solutions and SIN-1, alkaline conditions are often required to study the reactions of PN. When the strongly alkaline authentic PN solutions are added to buffered media, rapid decomposition of PN results in high concentrations of secondary radical species such as $^{\bullet}NO_2$ and $CO_3^{\bullet-}$. However, such rapid

burst of radicals fails to take into consideration the formation of pathological concentration of PN from rising levels of NO and $O_2^{\bullet-}$ in biological milieu [1,34]. Because changes in fluxes of these precursors can lead to very different product formations [31], we have utilized our two-component platform that generates a sustained flux of PN in a biomimetic fashion to explore the reactions of PN with tyrosine and tyrosine-containing peptides under different pH conditions, bicarbonate concentrations, and in the presence of thiols.

The biomimetic generation of PN from the two precursors in the wells of our multi-well platform is quite effective. Exposure of 1 mM of tyrosine to the ~4 μM per min flux of PN, generated for 30 min, afforded 46.5 μM of 3-NT (38.5 ± 0.4% nitration based on PN concentration). This yield is particularly notable when compared to ~1% tyrosine nitration obtained with 1 mM of SIN-1 (and comparable CO_2 concentration) after 12 h as reported by Mayer and coworkers [23]. Further, when a comparative study was performed where 1 mM tyrosine was exposed to 500 μM SIN-1 for 30 min in the presence of 1.25 mM $NaHCO_3$ (comparable to the free tyrosine study completed within the wells of the platform), the resulting absorbance spectrum lacked an absorption peak corresponding to 3-NT formation. It is important to note that the presence of urate in our wells does not appear to significantly attenuate the extent of tyrosine nitration. Presumably, both the steady and high concentration of PN and the slow reaction rate of PN with urate [2] give rise to this advantage in the present platform. Also, sustained release of NO, $O_2^{\bullet-}$, and PN within the wells avoids the use of rapid stirring to assure adequate exposure of a substrate to the RNS, as is required in studies where authentic PN is employed. The present PN-generating plate requires only undulation to promote uniformity throughout the wells. Further, because the well volume and respective sol-gel units can be easily adjusted to release desired concentrations of NO and $O_2^{\bullet-}$, our platform can release much higher

fluxes of PN compared to other two-component systems reported so far [23,25]. The metal nitrosyl employed in this platform releases NO significantly faster than alternative sources [23], and can match the relatively rapid release rate of $O_2^{\bullet-}$ from the xanthine oxidase system. When the flux ratio within the wells was adjusted to 1:2 (NO to $O_2^{\bullet-}$), the absorption band at 370 nm corresponding to 3-NT formation was absent in the electronic spectrum. This observation was expected because it has been established that when $O_2^{\bullet-}$ is in excess of NO, it reacts rapidly with $^{\bullet}NO_2$ to form peroxynitrate (O_2NOO^-) [35]. This anion rapidly decomposes to yield nitrite and molecular oxygen, thus inhibiting nitration of tyrosine. This control study effectively demonstrates the effectiveness of the platform to mimic *in vivo* scenarios where the flux of NO and $O_2^{\bullet-}$ can vary.

Because many NO donors are highly pH sensitive and only release optimal fluxes of NO under strict conditions, their use is restricted to limited pH ranges [36]. This feature impedes the utility of co-generative systems to study PN-dependent reactions under varied pH conditions. To circumvent this complication flow reactors have been employed where one or both of the PN precursors are flooded into a reaction vessel and a respective substrate is exposed to rapid bursts of saturated solutions of NO gas and/or alkaline KO_2 solutions [37]. In contrast, the light-controlled PN-generating platform employed in the present study allowed us to study the effects of pH on tyrosine nitration by PN without the use of flow reactor. When tyrosine was exposed to PN within the prefabricated wells of the platform under varied pH conditions, diminution in 3-NT formation was observed with increased acidity of the well milieu (pH = 7.4, 7.0, and 6.5, Table 1). In general, the process of tyrosine nitration is mediated by peroxynitrous acid (ONOOH) and nitrosoperoxocarbonate anion ($ONOOCO_2^-$) [1,2]. At physiological pH, PN is stabilized in its anionic form ($ONOO^-$) and reacts with CO_2 to form $ONOOCO_2^-$ [6,37].

However, as the pH drops (characteristic of local sites of inflammation) towards the pK_a of PN (6.8), the protonated form ONOOH predominates and inhibits the formation of $ONOOCO_2^-$ (Scheme 1) [2]. While both species are capable of inducing tyrosyl radical ($TyrO^{\bullet}$) formation to initiate the generation of 3-NT, superior specificity of strong oxidant carbonate radical ($CO_3^{\bullet-}$) generated from the homolytic cleavage of $ONOOCO_2^-$ (compared to the hydroxyl radical ($OH^{\bullet}$) generated from ONOOH) accounts for diminished nitration of tyrosine within the wells.

To further explore the nitration of tyrosine by PN within a peptide frame we designed a model peptide **Y1** with a single tyrosine residue and examined the extent of its nitration relative to nitration of free tyrosine. Exposure of **Y1** to ~4 μM per min flux of PN (under identical CO_2 concentration and pH value as in the case of free tyrosine) promoted very similar extent of nitration comparable to free tyrosine (percent nitration normalized to account for the concentration difference between free tyrosine and Y1). As discussed above, the presence and concentration of CO_2 mediates PN-dependent nitration through the formation of intermediate $ONOOCO_2^-$ that decomposes (homolytic) to yield $CO_3^{\bullet-}$ and $^{\bullet}NO_2$ at a rate of ~10^9 s^{-1} (Scheme 1) [38]. Indeed, alteration of CO_2 concentration within the wells of our platform resulted in significant modulation of 3-NT formation with **Y1** as the substrate. With a CO_2 concentration of ~100μM, a modest increase in nitration was observed compared to wells where no $NaHCO_3$ was incorporated (Table 2). However, when the concentration of CO_2 was approximately tripled, a significant increase in nitration was observed (~4.5 fold). These results verify $ONOOCO_2^-$-mediated nitration (characteristic of PN chemistry) of **Y1** within the wells of our platform.

Scheme 1 here

Following the successful nitration of tyrosine-containing peptide **Y1** under tightly controlled conditions, we sought out to observe the effect(s) of highly abundant antioxidant GSH on this PN-dependent nitration process. The addition of physiological concentrations of GSH to the wells of the platform where **Y1** was exposed to PN resulted in a slight *enhancement* of nitration. We assign this modest acceleration to the extended lifetime of NO in the presence of GSH within the wells of our platform. The photorelease of NO from the Mn(NO)•SG piece is fast compared to the initial release of $O_2^{\bullet-}$ from the XO/CAT•SG disk that requires diffusion of HX through the sol-gel matrix in the larger well. Therefore in the first minute or so of the experiment when the release rates are slightly unmatched, NO chemistry predominates and results in the nitrosylation of GSH [39,40]. The resulting S-nitrosylated glutathione product (S-nitrosoglutathione, GSNO) acts as a NO storage in the platform (much like in the body), extending the effective concentration of this precursor within the wells. This hypothesis is supported by mass spectral results of the well content where a peak corresponding to GSNO was observed (Fig. 3). Extension of the lifetime of NO in the wells by this route allows for a higher concentration of PN at the later part of the reaction and results in the moderately higher yield of nitrated product under such conditions.

The observed enhancement in nitration of **Y1** in the presence of thiol GSH (an *intermolecular* effect) prompted us to design a series of peptides **C1**, **CY1**, **CY2** and **CY3** to study *intramolecular* effects of thiols on the nitration of tyrosine within our platform. It has been proposed that the relative proximity of thiols and tyrosine residues within peptide and proteins can influence the extent of tyrosine nitration by PN and contribute to the general selectivity of this dynamic process through an intramolecular radical transfer pathway [41,42]. The presence of a cysteine residue spatially adjacent to a tyrosyl can act as a "radical sink," inhibiting nitration

process of the tyrosyl radical by $^{\bullet}NO_2$ and enhancing oxidation and S-nitrosylation of the thiol residue [43-46]. Interestingly, the sequence of radical-mediated modifications was indeed observed within the wells of the platform where **CY3** was exposed to PN. The extent of nitration at the tyrosine residue within **CY3**, where a cysteine and tyrosine residue were placed directly adjacent to each other, was significantly attenuated compared to the nitration observed in peptides **Y1**, **CY1**, and **CY2** (Table 3).

Mass spectral data collected from the **CY3** study contained peaks corresponding to 16 Da (−O), 30 Da (−NO), and 46 Da ($-NO_2$) mass additions to the parent peptide (Fig. 4). While the 30 Da and 46 Da mass additions (representing nitrosylation and nitration respectively) were observed in all three peptide studies, the relative intensity of the peaks varied. In the mass spectra of **CY1** and **CY2**, the 46 Da mass addition was the predominant peak, whereas in **CY3**, the 30 Da mass addition was observed to be significantly greater than the nitration peak. The electronic spectrum collected of the well content from the **CY3** study also showed a significant diminution of the absorbance band corresponding to the nitrated tyrosine ($\lambda_{\square\square\square}$= 370 nm), indicating that the 46 Da mass addition observed in the mass spectrum was largely a result of S-nitration of the cysteine residue within the peptide. The mass addition of 16 Da to the **CY3** peptide is a unique product that was not observed in **CY1** and **CY2** studies and likely corresponds to the oxidation of the thiol group to a sulfenic acid (−SOH). It is important to note here that the extent of nitration within peptide **CY1** and **CY2** (where the cysteine and tyrosine residues were 4 or 8 residues apart) were not significantly different (Table 3). Furthermore, the relative nitration of **CY1** and **CY2** was similar to that observed when **Y1** peptide was exposed to PN in the presence of GSH (Table 3). Taken together, the distinct products induced within the **CY3** peptide and the

dramatic attenuation in the extent of tyrosine nitration supports the intramolecular radical transfer process observed in other peptide and protein studies [47,48].

6. Conclusion

The present work demonstrates the utility of the two-component PN-generating platform as a convenient tool to study the reactions of PN with a wide range of substrates under controlled conditions including changes in pH. Previously, poor nitration yields induced *in situ* generated PN compared to yields generated upon exposure to authentic PN has been rationalized by Ingold and coworkers to be a result of varied rates of radical formations by the respective sources [34]. A rapid rate of NO photorelease from Mn(NO)•SG and careful matching of the flux ratio of NO and $O_2^{\bullet-}$ make this platform a valuable tool to study *the effects of continuous exposure of a substrate to PN*. The efficient nitration of tyrosine and tyrosine-containing peptides by physiologically relevant concentration of PN within the wells provide strong evidence in favor of the utility of this platform in future studies on PN chemistry.

Abbreviations

$CO_3^{\bullet-}$	carbonate radical
ESI-MS	electron spray ionization mass spectrometry
GSH	glutathione
GSNO	S-nitrosoglutathione
$GSNO_2$	S-nitrated glutathione
HOBt	hydroxybenzotriazole
HX	hypoxanthine;
(Mn(NO)	$[Mn(Papy_3)(NO)]ClO_4$
Mn(NO)•SG	Mn(NO)-encapsulated sol-gel;
$ONOOCO_2^-$	nitrosoperoxocarbonate anion;

PN, $ONOO^-$	peroxynitrite;
ONOOH	peroxynitrous acid;
PBS	phosphate buffer saline;
$O_2^{\bullet -}$	superoxide
$TyrO^{\bullet}$	tyrosyl radical;
XO/CAT•SG	xanthine oxidase/catalase-containing sol gel;
3-NT	3-nitrotyrosine.

Acknowledgements

This research was supported by a grant from the NSF (DMR-1105296). TdBM, RIP, and SOI acknowledge support from the IMSD grant GM-58903.

References

[1] P. Pacher, J.S. Beckman, L. Liaudet, Physiol. Rev. 87 (2007) 315-424.

[2] R. Radi, J. Biol. Chem. 288 (2013) 26464-26472.

[3] J.S. Beckman, W.H. Koppenol, Am. J. Physol. 271 (1996) C1424-C1437.

[4] C. Szabo, H. Ischiropoulos, R. Radi, Nat. Rev. Drug Discov. 8 (2007) 662-680.

[5] J.S. Beckman, J. Chen, H. Ischiropoulos, J.P Crow, Method Enzymol. 233 (1994) 229-240.

[6] G. Ferrer-Sueta, R. Radi, ACS Chem. Biol. 4 (2009) 161-177.

[7] S. Greenacre, H. Ischiropoulos, Free Rad. Res. 34 (2000) 541-581.

[8] P.H. Chan, J. Cerebr. Blood F. Met. 21 (2001) 2-14.

[9] R.M. Reynolds, W.R. Berry, I.L Binder, Biochemistry 44 (2005) 1690-1700.

[10] R.J. Lee, K.J. Kim, J.S. Lee, P.K. Kim, Arch. Pharm. Res. 32 (2009) 1109-1118.

[11] O. Cantoni, L. Palomba, A. Guidarelli, L. Tommasini, L. Cerioni, P. Sestili, Environ. Health Perspect. 110 (2002) 823-825.

[12] F. Torreilles, S. Salman-Tabcheh, M.C. Guerin, J. Torreilles, Brain Res. Rev. 30 (1999) 153-163.

[13] M.A. Smith, P.L. Richey Harris, L.M. Sayre, J.S. Beckman, G. Perry, J. Neurosci. 17 (1997) 2653-2657.

[14] H. Ischiropoulos, L. Zhu, J. Chen, M. Tsai, C.J. Martin, D.C. Smith, J.S. Beckman Arch. Biochem. Biophys. 298 (1992) 431-437.

[15] H. Ischiropoulos, L. Zhu, J.S. Beckman, Arch. Biochem. Biophys. 298 (1992) 446-451.

[16] J. S. Beckman, Chem. Res. Toxicol. 9 (1996) 836-844.

[17] R. Radi, Acc. Chem. Res. 46 (2013) 550-559.

[18] H. Ischiropoulos, Arch. Biochem. Biophys. 484 (2008) 117-121.

[19] R. Radi, Proc. Natl. Acad. Sci. USA 101 (2004) 4003-4008.

[20] A. van der Vliet, J.P. Eiserich, M.K. Shigenaga, C.E. Cross, Am. J. Respir. Crit. Care Med. 160, (1999) 1-9.

[21] C. Quijano, N. Romero, R. Radi, R. Free Rad. Biol. Med. 39 (2005) 728-741.

[22] M. Tien, B.S. Berlett, S. B., R.L. Levine, P.B. Chock, E.R. Stadtman, Proc. Natl. Acad. Sci. USA 96 (1999) 7809-7814.

[23] S. Pfeiffer, B. Mayer, J. Biol. Chem. 273 (1998) 27280-27285.

[24] C.D. Reiter, R.J. Teng, J.S. Beckman, J. Biol. Chem. 275 (2000) 32460-32466.

[25] S. Goldstein, G. Czapski, J. Lind, G. Merenyi, J. Biol. Chem. 275 (2000) 3031-3036.

[26] M.H. Papee, L.G. Petriconi, Nature. 204 (1964) 142-144.

[27] W.H. Koppenol, R. Kissner, J.S. Beckman, Method Enzymol. 269 (1996) 296-302.

[28] D. Gupta, B. Harish, R. Kissner, R., W.H. Koppenol, Dalton Trans. 29 (2009) 5730-5736.

[29] M.N. Alvarez, M. Trujillo, R. Radi, Method Enzymol. 359 (2002) 353-366.

[30] T. Sawa, T. Akaike, H. Maeda, J. Biol. Chem. 275 (2000) 32467-32474.

[31] T.R. DeBoer-Maggard, A. Resendez, P.K. Mascharak, ChemBioChem. 14 (2013) 2106-2109.

[32] K. Ghosh, A.A. Eroy-Reveles, B. Avila, T.R. Holman, M.M. Olmstead, P.K. Mascharak, Inorg. Chem. 43 (2004) 2988-2997.

[33] J. Zielonka, A. Sikora, J. Joseph, B. Kalyanaraman, J. Biol. Chem. 285 (2010) 14210-14216.

[34] G.R. Hodges, J. Marwaha, T. Paul, K.U. Ingold, Chem. Res. Toxicol. 13 (2000) 1287-1293.

[35] J.W. Coddington, J.K. Hurst, S.V. Lymar, J. Am. Chem. Soc. 121 (1999) 2438-2443.

[36] M. Feelisch, Arch. Pharmacol. 358 (1998) 113-122.

[37] M. Trujillo, M. Naviliat, M.N. Alvarez, G. Peluffo, G., R. Radi, Analusis. 28 (2000) 518-527.

[38] S. Carballal, S. Bartesaghi, R. Radi, Biochim. Biophys. Acta 1840 (2013) 768-780.

[39] J. S. Stamler, D.I. Simon, J.A. Osborn, M.E. Mullins, O. Jaraki, T. Michel, D.J. Singel, J. Loscalzo, Proc. Natl. Acad. Sci. 89 (1992) 444-448.

[40] B. Mayer, A. Schrammel, P. Klatt, D. Koesling, K. Schmidt. J. Biol. Chem. 270 (1995) 17355-17360.

[41] H. Zhang, J. Zielonka, A. Sikora, J. Joseph, Y. Xu, B. Kalyanaraman, (2009) Arch. Biochem. Biophys. 484 (2009) 134-145.

[42] H. Zhange, Y. Xu, J. Joseph, B. Kalyanaraman, J. Biol. Chem. 280 (2005) 40684-40698.

[43] A.A. Petruk, S. Bartesaghi, M. Trujillo, D.A. Estrin, D. Murgida, B. Kalyanaraman, M.A. Marti, R. Radi, Arch. Biochem. Biophys. 525 (2012) 82-91.

[44] P.S. Surdhar, D.A. Armstrong, J. Phys. Chem. 91 (1987) 6532-6537.

[45] B. Gaston, Biochim. Biophys. Acta 1411, (1999) 323-333.

[46] W.A. Prutz, H. Monig, J. Butler, E.J. Land, Arch. Biochem. Biophys. 243 (1985) 125-134.

[47] M.W. Foster, J.S. Stamler, J. Biol. Chem. 279 (2004) 25891-25897.

[48] S. Bhattacharjee, L.J. Deterding, J. Jiang, M.G. Bonini, K.B. Tomer, D.C. Ramirez, R.P. Mason, J. Am. Chem. Soc. 129 (2007) 13493-13501.

FIGURE LEGENDS

Fig. 1. The designed platform comprised of a $O_2^{\bullet-}$-generating sol-gel layer at the bottom of a well and NO-releasing sol-gel disc on top. It releases PN upon addition of HX and exposure of the plate to low power light.

Fig. 2. (**Left**) Mass spectrum of the well content collected after **Y1** was exposed to PN for 30 min. The two peaks highlighted in red correlate to the $[M+3H]^{3+}$ and $[M+Na]^{3+}$ of the nitrated Y1 peptide. Peak at 506 m/z corresponds to the $[M+3H]^{3+}$ peak of the unmodified parent peptide. The peak at 514 m/z represents $[M+Na]^{3+}$ of the parent peptide **Y1**. (**Right**) Electronic absorption spectrum of the well content. The absorbance band (λ_{max}= 370 nm) highlighted in red corresponds to the absorption band of the nitrated tyrosine residue within **Y1**.

Fig. 3. Partial mass spectrum collected from the well content where **Y1** was exposed to PN in the presence of GSH, highlighting the region with peaks corresponding to GSH (307 m/z, $[M+H]^+$, 330 m/z, $[M+Na]^+$) and its nitrosylation adduct GSNO (360 m/z, $[M+Na]^+$).

Fig. 4. (**Left**) Mass spectrum of the well content collected after **CY3** was exposed to PN for 30 min. The mass spectral data showed mass additions of 16 Da, 30 Da, and 46 Da corresponding to possible peaks 745 m/z (green), 749 m/z (blue), and 755 m/z (red), respectively. The second red-labeled peak at 762 m/z corresponds to the addition of a nitro group and pairing of the resulting **CY3** peptide with Na. (**Right**) Structures representative of the potential products associated with the observed additions in the mass spectrum.

Fig. 5. Electronic absorption spectrum of **CY1** peptide in the presence of NO (blue dashed line), $O_2^{\bullet -}$ (green dotted line) and PN (red solid line)

Scheme 1. The reaction and decomposition rates of critical primary and secondary radicals mediated by PN

FIGURE 1

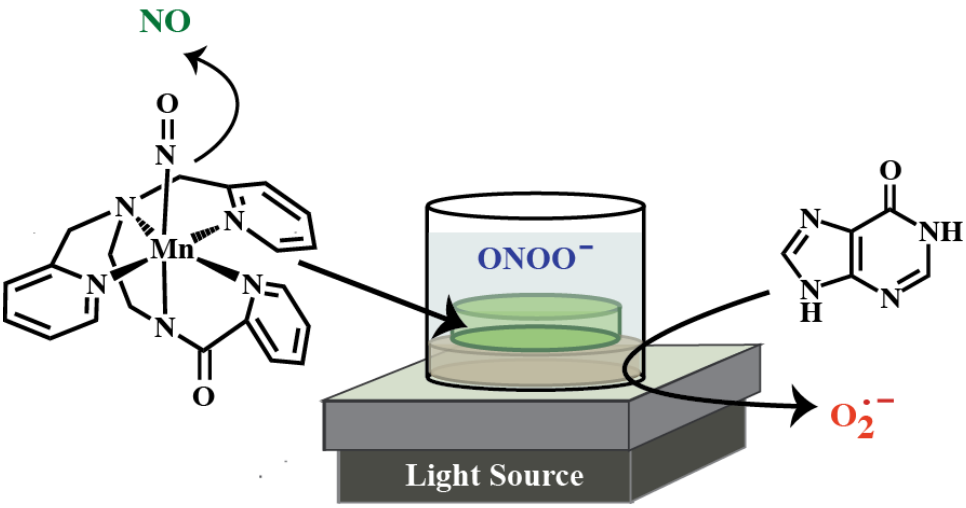

FIGURE 2

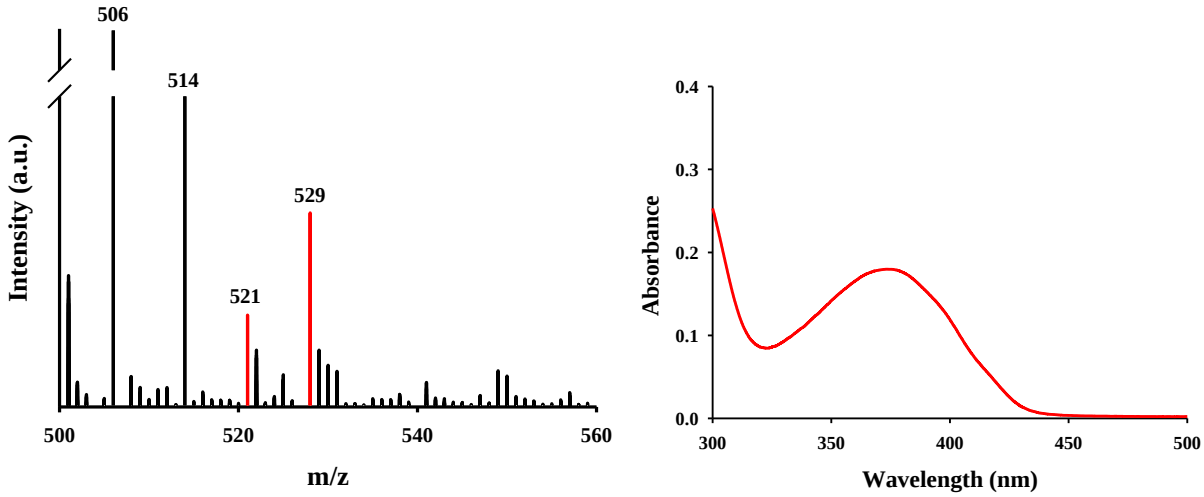

FIGURE 3

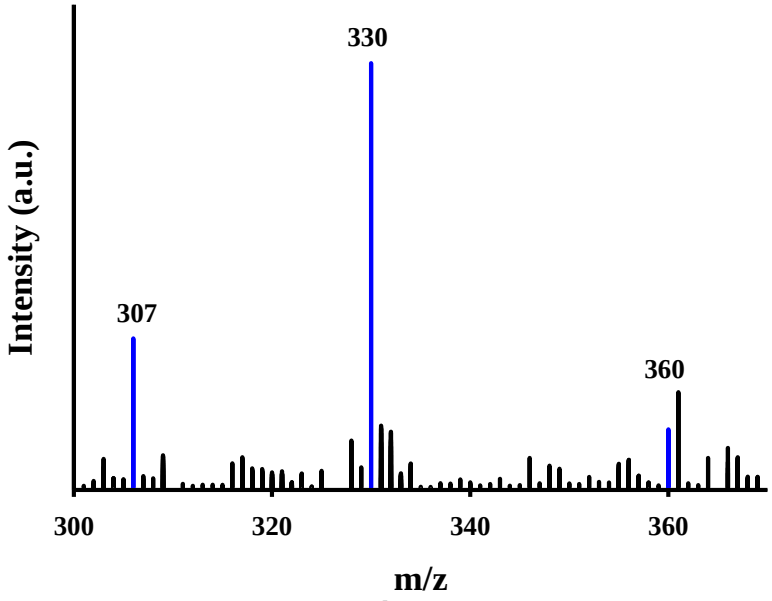

FIGURE 4

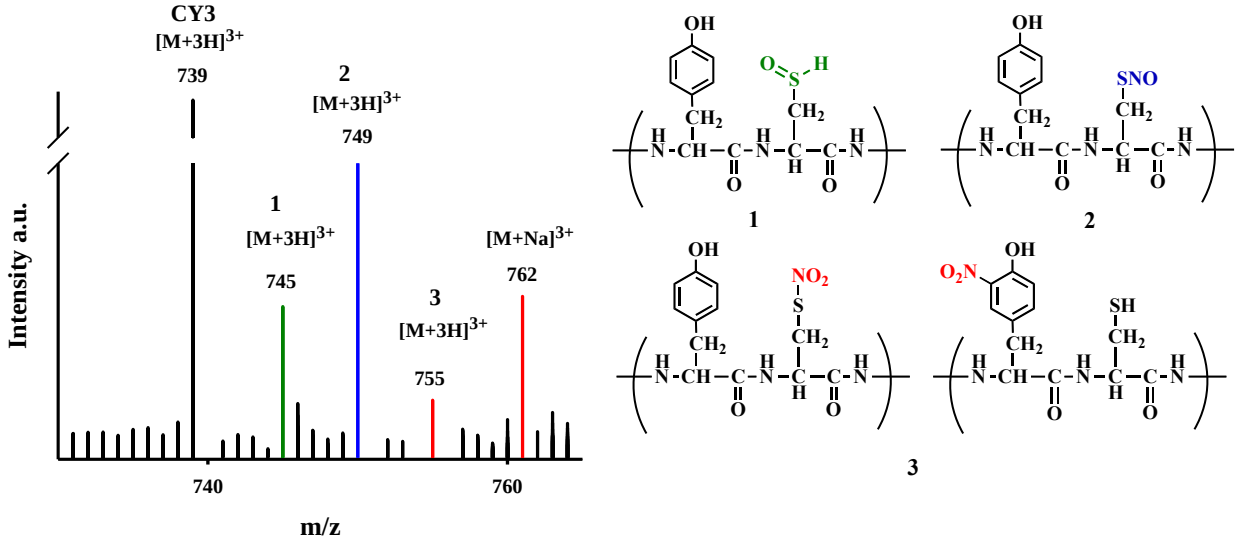

FIGURE 5.

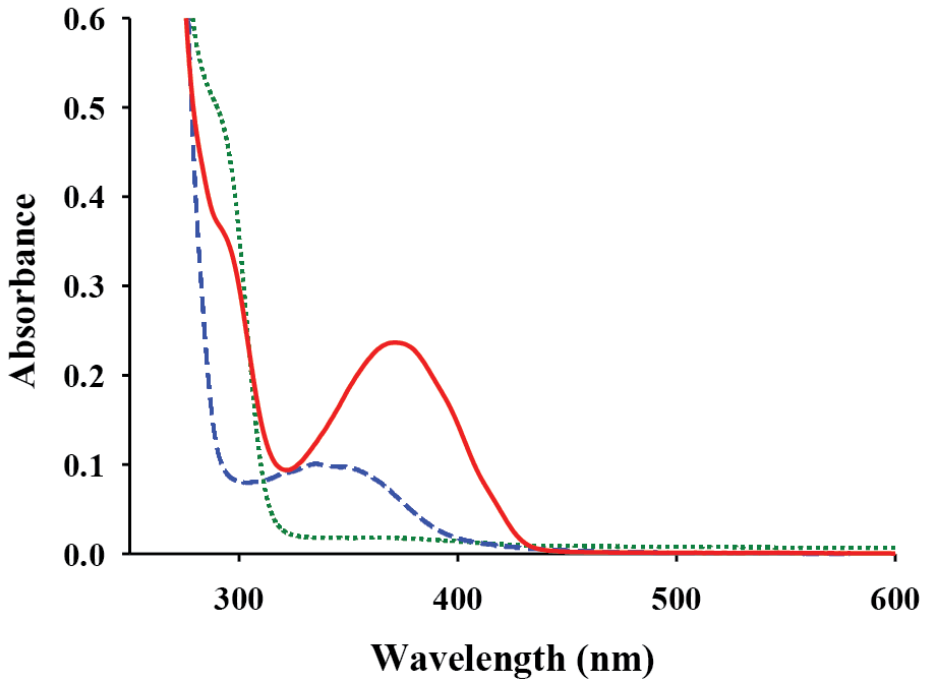

SCHEME 1

$$ONOO^- + CO_2 \longrightarrow ONOOCO_2^- \qquad k = 4.6 \times 10^4\ M^{-1}s^{-1} \quad [37]$$

$$ONOOCO_2^- \longrightarrow CO_3^{\bullet -} + {}^{\bullet}NO_2 \qquad k = 6.5 \times 10^8\ s^{-1} \quad [21]$$

$$ONOOH \longrightarrow NO_3^- + H^+ \qquad k = 0.63\ s^{-1} \quad [37]$$

$$ONOOH \xrightarrow{k = 0.27\ s^{-1}\ [37]} {}^{\bullet}OH + {}^{\bullet}NO_2$$

Pictogram

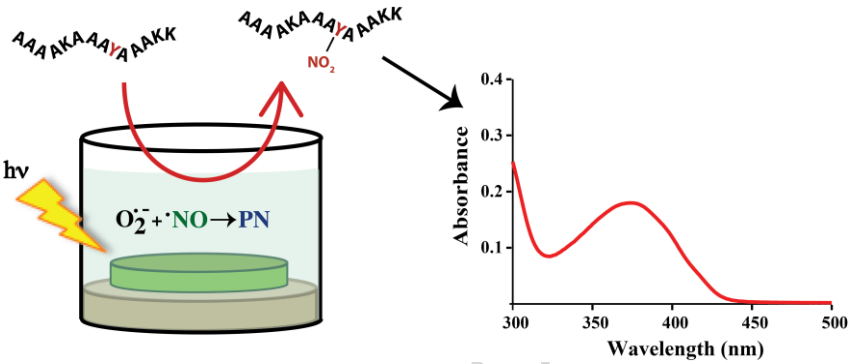

Synopsis for Graphical Abstract

Highly efficient nitration of tyrosine in model peptides has been achieved under varied pH, CO_2 and thiol concentrations within the wells of a peroxynitrite-generating platform controlled by light. Placement of a neighboring cysteine residue strongly attenuates the effects of peroxynitrite on tyrosine.

TABLES

Table 1. Percent nitration of tyrosine under various pH conditions

(Values calculated based on total PN concentration)

Sample	pH	Percent Nitration
Tyrosine	7.4	38.5 ± 0.4 %
Tyrosine	7.0	30.4 ± 0.4 %
Tyrosine	6.5	22.2 ± 0.3 %

Table 2. Percent nitration of **Y1** at pH 7.4 under various $NaHCO_3$ concentrations

(Values calculated based on total PN concentration)

Sample	Percent Nitration	[$NaHCO_3$]
Y1	2.8 ± 0.5 %	0 mM
Y1	7.7 ± 0.9 %	1.25 mM
Y1	37.2 ± 1.1 %	4.0 mM

Table 3. Intramolecular effects of cysteine on nitration of tyrosine in designed peptides

(Values calculated based on total PN concentration)

Peptide	Sequence	Percent Nitration
CY1	AAA**C**AAAKKAAA**Y**AAAKK	39.1 ± 1.5 %
CY2	AAAKAAA**C**KAAA**Y**AAAKK	41.7 ± 1.8 %
CY3	AAAKKAAA**CY**AAAKK	4.8 ± 0.7 %